

Scalarized compact objects in a vector-tensor Horndeski gravity

Y. Brihaye[†] *and* Y. Verbin[‡]

[†]Physique-Mathématique, Université de Mons, Mons, Belgium

[‡]Department of Natural Sciences, The Open University of Israel, Raanana 4353701, Israel

April 10, 2020

Abstract

We have discovered a new type of scalarized charged black holes in a surprisingly simple system: an Einstein-Maxwell-Klein-Gordon field theory where the three fields couple non-minimally through a Horndeski vector-tensor term. In addition to hairy charged black holes, this system exhibits Horndeski-Reissner-Nordstrom solutions and ordinary Reissner-Nordstrom ones which bifurcate to the scalarized solutions. There exist also vector-tensor regular solutions with naked singularities. We analyze the solutions and present their main features.

1 Introduction

In the gigantic effort aimed to understand the dark matter and dark energy problems of the Universe, numerous extensions of General Relativity (GR) have been studied in the last few decades. Among these generalized gravities the extensions of the minimal Einstein-Hilbert lagrangian by scalar and/or vector fields play an important role. With the main objective of maintaining field equations of the second order in derivatives, the works of G. Horndeski [1, 2] provoked a considerable revival of interest in the last years. Apart from cosmological considerations, the non-minimal geometric gravities of space-time extended by extra fields leads to the possibility to evade the limitation of classical solutions due to no-hair theorems [3, 4, 5] valid in the Einstein-Hilbert theory. A rich set of new compact objects – hairy black holes (HBH), boson stars and wormholes – can be constructed in some extended gravities. But very surprisingly, black holes with scalar hair were found to exist even with minimal coupling only: Attracting a lot of attention, a family of hairy black holes (HBH) was first obtained in [6] within the Einstein gravity minimally coupled to a complex scalar field. In this case, the no-hair theorems [3, 4, 5] are bypassed by the rotation of the black hole and the synchronization of the spin of the black hole with the (internal) angular frequency of the scalar field. Reviews on the topic of black holes with scalar hairs are provided e.g. in [7, 8, 9]. The scalar-tensor theory of [1] was revived in the context of Galileon theory [10] and its extensions in [11]. The general lagrangian of scalar tensor gravity is very rich and special cases were studied by several authors. In many of these studies the Gauss-Bonnet geometric invariant plays a central role; although in four dimension the Gauss-Bonnet term is a pure divergence, it is rendered non trivial by a coupling to the scalar field through a function $H(\phi)$. The truncation of the Galileon theory to lagrangians admitting a shift symmetric scalar field was worked out by Sotiriou and Zhou [12] with a linear function $H(\phi)$. Static spherically-symmetric hairy black holes were

constructed numerically and perturbatively in [13]. Abandonning the hypothesis of shift symmetry, several groups [14, 15, 16] considered during the past year, new types of non-minimal coupling terms between a scalar field and specific geometric invariants (essentially the Gauss-Bonnet term). In these models the occurrence of hairy black holes results from an unstable mode associated to the scalar field equation (a generalized Klein-Gordon equation) in the background of the underlying metric (the probe limit). The coupling constant characterizing the interaction between the scalar field and the geometric invariant plays a role of a spectral parameter of the linear equation. We use to say that the hairy black holes appear through a *spontaneous scalarization* for a sufficiently large value of the coupling constant. Away from black holes, it was demonstrated in [17] that the energy momentum tensor associated with a GB term also violate the energy condition, opening the door for constructing wormhole in Einstein-Gauss-Bonnet models coupled to normal matter field. Such objects were indeed constructed in [18] and in [19] where the properties, domain of existence and stability were studied in detail for some choices of the coupling function $H(\phi)$. In a series of recent papers [20, 21], other types of extensions of the Einstein-Hilbert-Maxwell lagrangians have been presented and families of charged hairy black holes have been constructed with a non-minimal coupling of the scalar field to the electromagnetic Maxwell-Faraday.

So far, up to our knowledge, no analogous investigation was done for the vector-tensor Horndeski theory [2] extended by a scalar field. The original vector tensor theory proposed in [2] is characterized by a single interacting term between the geometry and the vector field with a single coupling constant. The generic static, spherically symmetric solutions are essentially deformations of the Reissner-Nordstrom solutions. These Horndeski-Reissner-Nordstrom (HRN) black holes were studied in detail in [22].

In this paper we reconsider the Horndeski vector-tensor lagrangian and we extend it by a real scalar field coupled, again, to the Horndeski interaction term by means of a coupling function $H(\phi)$. In this new type of scalar-vector-tensor theory, we have constructed soliton-like solutions and hairy black holes that bifurcate from the solutions of [22] at specific values of the coupling constants. The paper is organized as follows: in Sec. 2 we present the model and in Sec. 3 the field equations and appropriate boundary conditions. In Sec. 4 we present the black holes of the vector-tensor system and in Sec. 5 we arrive at the main subject of this paper, the charged black holes with scalar hair. A summary of the results and some perspectives are the objective of Sec. 6.

2 The model

We are interested in classical solutions associated with Einstein-Maxwell-Klein-Gordon lagrangian extended by a non-minimal coupling term inspired by the work of G. Horndeski. The action considered is of the form

$$S = \int d^4x \sqrt{-g} \left[\frac{1}{2\kappa} R - \frac{1}{2} \nabla_\mu \phi \nabla^\mu \phi - \frac{1}{4} F_{\mu\nu} F^{\mu\nu} + H(\phi) \mathcal{I}(g, A) \right] \quad (2.1)$$

where R is the Ricci scalar, $F_{\mu\nu}$ in the electromagnetic field strength and ϕ represents a real scalar field. We use $\kappa = 8\pi G$ which we later take to be 1 by rescaling. The last term $\mathcal{I}(g, A)$ is the non-minimal coupling of the vector field to the geometry introduced by Horndeski [2] as a possible

interaction term which keeps the field equations of second order.

$$\mathcal{I}(g, A) = -\frac{1}{4}(F_{\mu\nu}F^{\kappa\lambda}R^{\mu\nu}{}_{\kappa\lambda} - 4F_{\mu\kappa}F^{\nu\kappa}R^{\mu}{}_{\nu} + F_{\mu\nu}F^{\mu\nu}R). \quad (2.2)$$

Following the spirit of many recent works, the vector-tensor gravity lagrangian has been augmented by a real scalar field ϕ and this scalar is coupled to the Horndeski interaction term via the coupling function $H(\phi)$. The case of a constant $H(\phi)$ then corresponds to the original vector-tensor Horndeski lagrangian.

Recently, several hairy black holes have been constructed in other versions of the model of the type (2.1) above, mainly by choosing for $\mathcal{I}(g)$ the Gauss-Bonnet invariant or the Faraday-Maxwell term $\mathcal{I}(A) = F_{\mu\nu}F^{\mu\nu}$. In these works several forms of the function $H(\phi)$ were used in order to construct uncharged hairy black holes, see e.g. [14, 15, 16, 23] as well as charged ones [24]. Here we will take the ‘‘tripartite’’ coupling term and show that it produces a rich and interesting family of compact objects.

3 Spherically-symmetric solutions

3.1 Ansatz

In order to obtain static spherically symmetric solutions we will adopt a metric of the form

$$ds^2 = -f(r)a^2(r)dt^2 + \frac{1}{f(r)}dr^2 + r^2d\Omega_2^2 \quad (3.1)$$

completed by a spherically-symmetric scalar field $\phi(x^\mu) = \phi(r)$ and a spherically-symmetric electric field derived from the vector potential $A_0 = V(r)$, $A_{1,2,3} = 0$.

Substituting the ansatz in the field equations, the system can be reduced to a set of four non linear differential equations for the functions $f(r)$, $a(r)$, $V(r)$ and $\phi(r)$ (with the notation $H'(\phi) = dH/d\phi$):

$$(r^2af\phi')' + \frac{H'(\phi)(1-f)(V')^2}{a} = 0 \quad (3.2)$$

$$\left[\frac{(r^2 + 2H(\phi)(1-f))V'}{a} \right]' = 0 \quad (3.3)$$

$$1 - f - rf' = \frac{\kappa r^2}{2} \left[f\phi'^2 + \frac{(r^2 + 2H(\phi)(1-f))(V')^2}{r^2a^2} \right] \quad (3.4)$$

$$\frac{ra'}{a} = \frac{\kappa r^2}{2} \left(\phi'^2 + \frac{2H(\phi)(V')^2}{r^2a^2} \right) \quad (3.5)$$

The potential $V(r)$ can be eliminated by using the Maxwell equation (the full equations depend on V' only), leading to

$$V'(r) = \frac{Qa(r)}{r^2 + 2H(\phi(r))(1-f(r))} \quad (3.6)$$

where Q is the integration constant which we interpret as the electric charge of the solution. Without loss of generality, we will assume $Q \geq 0$. With this elimination, the three final equations

are of the first order for the functions $f(r)$, $a(r)$ and of the second order for $\phi(r)$. They depend on the charge parameter Q and the shape of the scalar coupling function $H(\phi)$. For the initial study of this work we take the simple choice

$$H(\phi) = \gamma + \alpha\kappa\phi^2 \quad (3.7)$$

where α , γ are independent coupling constants. This parametrization contains the case of $\alpha = 0$ which corresponds to the original vector-tensor Horndeski lagrangian and $\gamma = 0$ with $\alpha > 0$ which as we will see, produces scalarized black holes. The system depends therefore on the coupling constants α and γ and the charge parameter Q .

3.2 Boundary conditions and asymptotics

For a fixed choice of α, γ and Q , four conditions on the boundary need to be fixed to specify a solution. Because we look for localized, asymptotically flat solutions, we require

$$a(r \rightarrow \infty) = 1 \quad , \quad \phi(r \rightarrow \infty) = 0 \quad , \quad m(r \rightarrow \infty) = M \quad (3.8)$$

where we define the mass function by

$$f(r) = 1 - \frac{2m(r)}{r} \quad (3.9)$$

and M is a positive constant. For black hole solutions, imposing a regular horizon at $r = r_h$ needs $f(r_h) = 0$. The equation of the scalar field is then singular in the limit $r \rightarrow r_h$; obtaining regularity requires a very specific relation between the values $\phi(r_h)$ and $\phi'(r_h)$. Examining the equations the conditions for a regular scalarized black hole at r_h turn out to be :

$$f(r_h) = 0 \quad , \quad \phi'(r_h) = \frac{2Q^2 H'}{r(2H + r^2)(\kappa Q^2 - 2r^2 - 4H)} \Big|_{r=r_h} \quad . \quad (3.10)$$

The boundary value problem is then fully specified by (3.8) and (3.10). Existence of an hairy black hole will imply in addition setting a value $\phi(r_h) \neq 0$ for the scalar field; this clearly leads to a relation between the constants α , γ , Q and $\phi(r_h)$. Stated differently, for any α and γ , the value of $\phi(r_h)$ fixes the values of the charge Q or vice-versa. In addition to the electric charge Q , the solutions will be further characterized by the mass M , scalar charge D , the temperature $T_H = a(r_h)f'(r_h)/(4\pi)$ and the horizon area $A_H = 4\pi r_h^2$. Using the field equations for $r = r_h$ we find the explicit equation for the temperature:

$$T_H = \frac{a(r_h)(2r_h^2 + 4H(\phi_h) - \kappa Q^2)}{8\pi r_h(r_h^2 + 2H(\phi_h))} \quad . \quad (3.11)$$

4 HRN black holes and regular solutions

4.1 Reissner-Nordstrom solutions

In the absence of the scalar field and the non-linear Horndeski term, the generic solutions are the Reissner-Nordstrom (RN) black holes

$$f(r) = 1 - \frac{r_h^2 + \kappa Q^2/2}{r_h r} + \frac{\kappa Q^2}{2r^2} \quad , \quad a(r) = 1 \quad , \quad V(r) = -\frac{Q}{r} \quad (4.1)$$

The outer horizon is situated at $r = r_h$ and is simple for $0 \leq \kappa Q^2 < 2r_h^2$. The mass and temperature of these black holes are respectively $M = (2r_h^2 + \kappa Q^2)/(4r_h)$ and $T_H = (2r_h^2 - \kappa Q^2)/(8\pi r_h^3)$. The horizon becomes double for $\kappa Q^2 = 2r_h^2$ corresponding to an extremal black hole. For the future discussion, let us point out that these extremal black holes have $M = r_h = \sqrt{\kappa/2} Q$ so that $\sqrt{\kappa}Q/M = \sqrt{2}$, irrespectively of r_h .

4.2 HRN black holes

If the non-minimal coupling of the Horndeski term is present, but the scalar field is still absent (i.e. $H(\phi) = \gamma$ - see Eq. (3.7)), the solutions are deformations of the Reissner-Nordstrom solutions [22]. To first order in the non minimal coupling constant γ , we found the following asymptotic behaviour

$$f(r) = 1 - \frac{2m(r)}{r} \quad , \quad m(r) = M - \frac{\kappa Q^2}{4r} + \frac{\gamma \kappa Q^2 M}{4r^4} + \dots \quad (4.2)$$

$$a(r) = 1 - \frac{\gamma \kappa Q^2}{4r^4} + \dots \quad , \quad V(r) = -\frac{Q}{r} + \frac{\gamma M Q}{r^4} + \dots \quad (4.3)$$

These solutions were already studied in [22], so we will be brief here, although our method is somewhat different. We solved the system by using the numerical routine COLSYS [25] as will be described in more details in Sec. 5.1. In the numerical construction of solutions we took advantage of the freedom to rescale the radial coordinate r as $r/r_h \rightarrow r$ so the horizon is located at $r = 1$ for all black hole solutions. The electromagnetic potential A_μ the charge Q and the mass M are rescaled accordingly to become dimensionless in such a way that we may set $\kappa = 8\pi G = 1$. The coupling constant γ becomes dimensionless as well. In what follows we will not distinguish in most cases between rescaled and non-rescaled quantities. It can be inferred from the context which of those we mean.

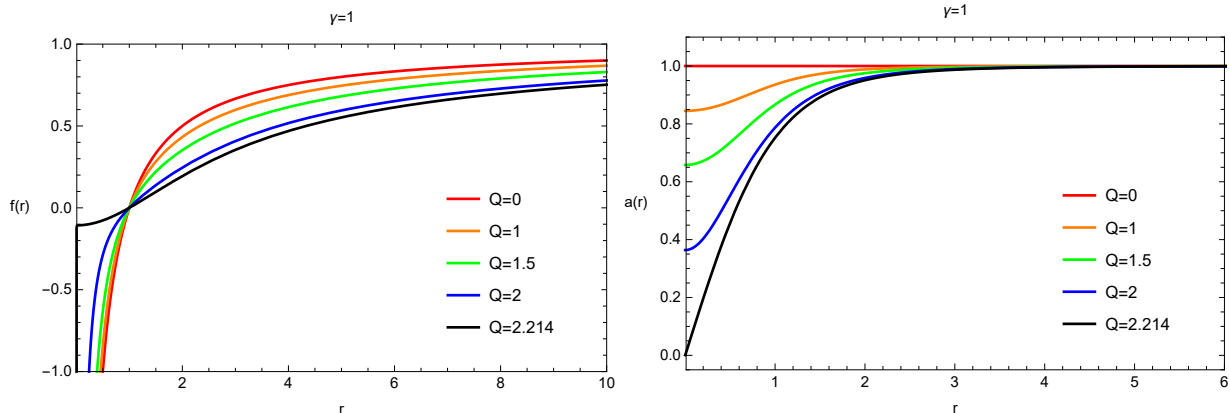


Figure 1: Several profiles of HRN black hole solutions characterized by Q from $Q = 0$ (Schwarzschild) to the maximal possible $Q = 2.214$ for $\gamma = 1$. Note that the figure includes the region inside the horizon which is for all solutions at $r = 1$.

We present in Fig. 1 several generic profiles of these Horndeski-Reissner-Nordstrom black holes. The black hole solutions for a given value of γ are characterized by the electric charge as shown

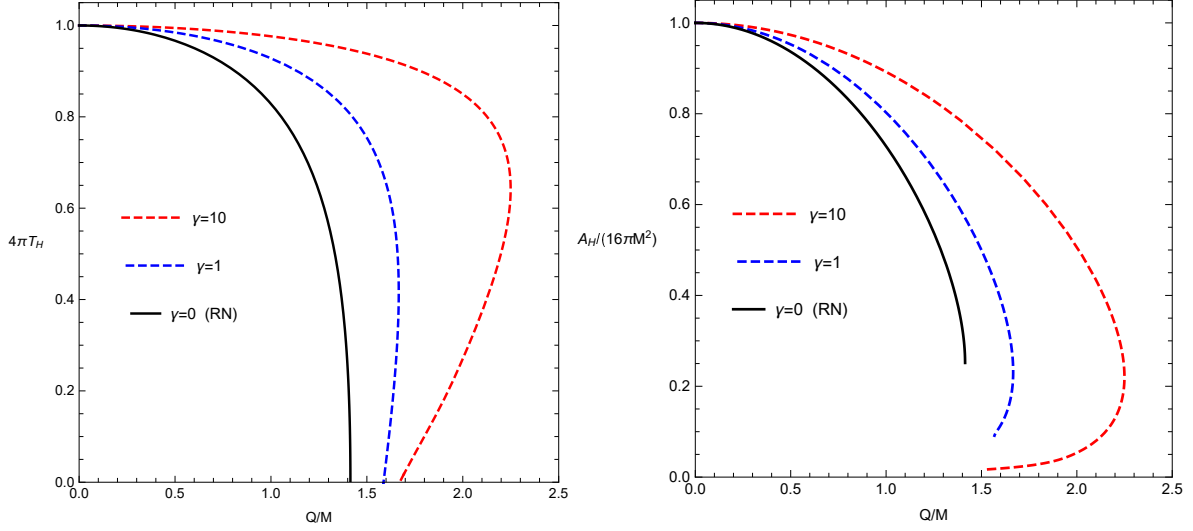


Figure 2: The temperature and horizon area as function of Q/M for the RN (solid lines) and HRN black holes with $\gamma = 1, 10$ (dashed lines). Left: Temperature. Right: The ratio $A_H/16\pi M^2$.

clearly in Fig. 1. For any γ the charge is limited to a finite interval $0 \leq Q \leq Q_{max}(\gamma)$ which exceeds the RN limit of $\sqrt{\kappa}Q/M = \sqrt{2}$ mentioned above.

In Figure 2 we demonstrate the behavior of the temperature and horizon area as a function of the charge to mass ratio Q/M .

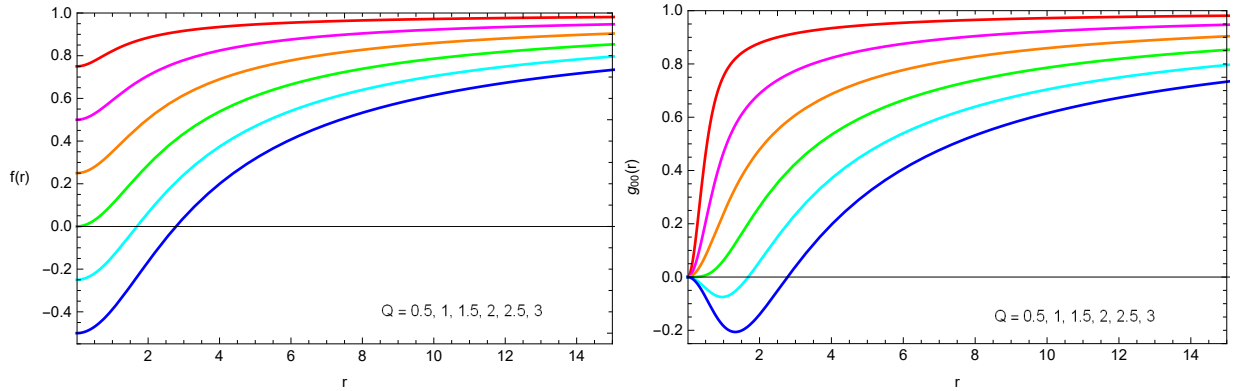


Figure 3: Several profiles of regular solutions of the Horndeski vector-tensor system for $0 < \bar{Q} < 3$. The curves with the lower $f(0)$ correspond to the larger \bar{Q} - values.

4.3 HRN regular solutions

In addition, we have found a new family of vacuum solutions of this system which are regular for $r > 0$ and exhibit a naked singularity since $a(0) = 0$. The singularity is evident as the Ricci and Kretschmann invariants diverge as $r \rightarrow 0$. These solutions solve Eqs (3.3)-(3.5) with $\phi(r) = 0$ and

$H(\phi) = \gamma$ and satisfy the following conditions at the origin:

$$m(0) = 0 \quad , \quad f(0) = 1 - 2m'(0) = 1 - \sqrt{\frac{\kappa}{\gamma}} \frac{Q}{2} \quad , \quad a(0) = 0 \quad (4.4)$$

These solutions are parametrized by the rescaled electric charge $\bar{Q} = \sqrt{\kappa/\gamma} Q$ which is the only free parameter for this kind of solutions. The regular solutions are divided into two subclasses: the first contains the solutions for which $f(r) > 0$ everywhere. These solutions exist in the charge interval $0 < \sqrt{\kappa/\gamma} Q < 2$ which corresponds to $f(0) > 0$. The solutions of the second subclasses exhibit a horizon where $f(r_h) = 0$ and $f(r) < 0$ but finite for $r < r_h$. These solutions exist for $\sqrt{\kappa/\gamma} Q > 2$. Fig. 3 depicts the metric functions $f(r)$ and $g_{00}(r) = f(r)a(r)^2$ of the solutions of both subclasses.

5 Black holes with scalar hair

5.1 Physical parameters

The main result of this work is the demonstration of the scalarized HRN black holes.

These hairy black holes can be characterized by their mass M , electric charge Q and scalar charge D , related respectively to the asymptotic decay of the functions $m(r)$ (or $f(r)$), $V(r)$ and $\phi(r)$. The asymptotic behavior is:

$$\begin{aligned} m(r) &= M - \frac{\kappa(Q^2 + D^2)}{4r} - \frac{\kappa MD^2}{4r^2} + \frac{\kappa D^2(\kappa Q^2 - 8M^2)}{24r^3} - \frac{\kappa MD^2(48M^2 - 12\kappa Q^2 - \kappa D^2)}{96r^4} + \dots \\ a(r) &= 1 - \frac{\kappa D^2}{4r^2} - \frac{2\kappa MD^2}{3r^3} - \frac{\kappa D^2(48M^2 - 4\kappa Q^2 - 3\kappa D^2)}{32r^4} + \dots \end{aligned} \quad (5.1)$$

$$\begin{aligned} V(r) &= -\frac{Q}{r} + \frac{\kappa Q D^2}{12r^3} + \frac{\kappa M Q D^2}{6r^4} + \dots \\ \phi(r) &= \frac{D}{r} + \frac{MD}{r^2} + \frac{D(16M^2 - 2\kappa Q^2 - \kappa D^2)}{12r^3} + \frac{MD(12M^2 - 3\kappa Q^2 - 2\kappa D^2)}{6r^4} \dots \end{aligned} \quad (5.2)$$

The temperature $T_H = a(r_h)f'(r_h)/(4\pi)$ further characterizes the solutions. Note that the scalar charge D is an independent charge and is not fixed by M and Q . The non-minimal coupling constant appears explicitly only in the higher order terms of the asymptotic expansion, but its effect is of course evident from non-vanishing scalar charge. This is also the reason why the limit $D \rightarrow 0$ does not lead from Eqs. (5.1)–(5.2) to Eqs. (4.2)–(4.3).

Since the non-linear equations do not admit closed form solutions, we solved the system by using the numerical routine COLSYS [25]. It is based on a collocation method for boundary-value differential equations and on damped Newton-Raphson iterations. The equations are solved with a mesh of a few hundred points and relative errors of the order of 10^{-6} . Various checks on the solutions were performed by obtaining them independently using the MATHEMATICA package.

In the numerical construction of solutions we took advantage of a rescaling of the radial coordinate r and of the matter fields ϕ, A_μ to set $\kappa = 8\pi G = 1$ and $r_h = 1$. The coupling constant α becomes dimensionless as well. Accordingly, the regularity conditions (3.10) take the form:

$$f(1) = 0 \quad , \quad \phi'(1) = \frac{4Q^2\alpha\phi(1)}{(2\alpha\phi(1)^2 + 1)(Q^2 - 2 - 4\alpha\phi(1)^2)} \quad (5.3)$$

where we used the further simplification to construct black hole solutions in the case $\gamma = 0$ only. From now on we assume $H(\phi) = \alpha\phi^2$.

5.2 Probe limit

Before attacking the construction of hairy black holes, it is useful to study the equation of the scalar field in the background of a RN black hole, that is to say that we first solve the Klein-Gordon equation sourced by the non-minimal coupling term. Since we assume $H = \alpha\phi^2$ the equation is linear and of the form :

$$(r^2 a f \phi')' = \alpha W \phi \quad , \quad W(r) \equiv -2(1 - f(r))(V')^2/a(r). \quad (5.4)$$

It turns out that for values of Q such that $0 \leq Q \leq \sqrt{2}$ this equation admits one critical value of the coupling constant, say $\alpha(Q)$, for which the equation admits a regular, localized, nodeless solution for ϕ . (Note: higher critical values of α exist with eigenfunction ϕ presenting one or several modes exist as well but we do not report them here). The relation between α and Q is presented on the left side of Fig. 4; the profile of the potential $W(r)$ and the corresponding eigenfunction $\phi(r)$ are shown on the right side of the figure for two values of Q and setting $r_h = 1$. As known from previous studies, the existence of such solutions constitutes an evidence for a tachyonic instability of the RN solution in the presence of a scalar field and leads to a bifurcation of hairy black holes from the RN solutions. We use to say that the hairy solutions “appear spontaneously” $Q > Q(\alpha)$.

5.3 Hairy black holes

Since we found regular, localized, nodeless solutions to the scalar field equation in the probe limit, we proceed to solving the full system, Eqs (3.2) – (3.5). As mentioned above, we solved the system numerically, and we now discuss the pattern of solutions in the space of the parameters α and Q . We limit the presentation to solutions with no node of the function ϕ and insist on solutions with

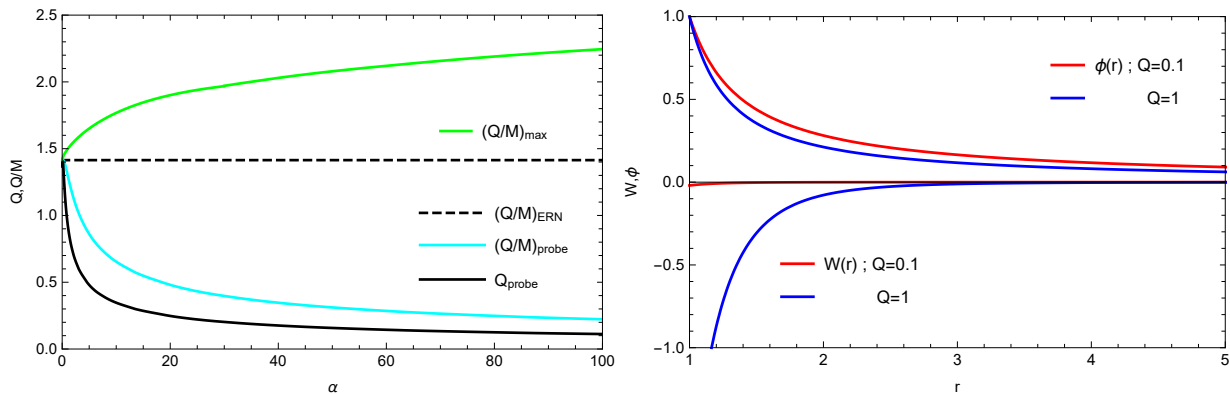


Figure 4: Left: The domain of existence of spherical hairy black holes in the $(\alpha, Q/M)$ plane: they exist between the blue and the red Q/M lines. The line $(Q/M)_{ERN} = \sqrt{2}$ for the extremal RN solution is added as a reference. The curve of Q vs. α of the probe limit corresponds to the line along which exist regular, localized, nodeless $\phi(r)$. Right: The “potential” $W(r)$ and the eigenmode $\phi(r)$ (normalized to $\phi(r_h) = 1$) for two values of the charge Q .

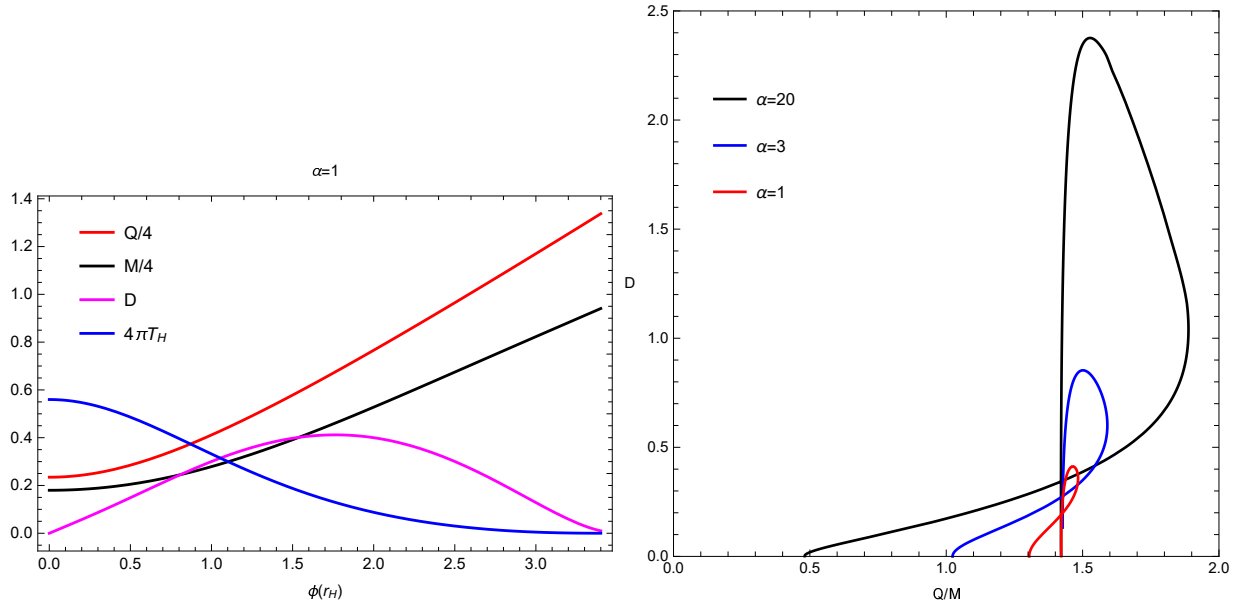


Figure 5: Left: The dependence on the horizon value of the scalar field of mass, electric charge, scalar charge and temperature of the HBH corresponding to $\alpha = 1$. Right: Three curves of HBH scalar charge D vs. Q/M for three values of α : $\alpha = 1, 3, 20$.

$\phi(r) \rightarrow 0$ rather than approaching a non-zero constant which exist as well. Technically the solutions are constructed by fixing the parameter α and increasing gradually the value $\phi(r_h)$; for a choice of these parameters an hairy black hole (HBH) exists just for a very specific value of the charge, i.e. $Q = Q(\alpha, \phi(r_h))$. The data corresponding to the typical value $\alpha = 1$ is plotted on the left hand side of Fig. 5. We see that solutions exist from vanishingly small $\phi(r_h)$ up to a maximal value of $\phi(r_h)$ and for all solutions $Q > M$. The temperature decreases monotonically with $\phi(r_h)$, while the scalar charge D vanishes at both ends and has a maximum at a certain point in the middle.

On the right hand side of Fig. 5 three curves of the scalar charge D versus the dimensionless ratio Q/M appear for $\alpha = 1, 3, 20$. The loop structure results from the non-monotonic dependence of D and Q/M on $\phi(r_h)$.

The behavior of the temperature and horizon area of HBH is shown in Fig. 6. The temperature and the reduced horizon area $a_h \equiv A_H/16\pi M^2$ are plotted versus the dimensionless ratio Q/M for $\alpha = 1, 3, 20$ as well as for the RN family ($\alpha = 0$). The branches of HBH bifurcate from the RN curve respectively for $Q \approx 0.94$, $Q \approx 0.605$ and $Q \approx 0.26$. The curves of T_H and a_h versus Q/M actually represent two families of HBH, merging at a maximal value of the parameter Q/M which increases with α . The solutions correspond to different intervals of $\phi(r_h)$: small and large. The solutions with small $\phi(r_h)$ bifurcate from the RN forming the upper branch (i.e. larger T_H and a_h). The second branch corresponds to larger values of $\phi(r_h)$ (typically $\phi(r_h) \sim 3.0$) and terminates at $Q/M = \sqrt{2}$, irrespectively of the value of coupling constant α (an explanation of this feature will come later). The figure further reveals that, on the whole region where RN and HBH coexist, the reduced horizon area $a_h \equiv A_H/16\pi M^2$ is larger in the case of the hairy solutions. Invoking the Bekenstein-Hawking black hole entropy formula, it turns out that the HBH are *entropically preferred* with respect to RN black holes. This feature seems to be common with HBH constructed

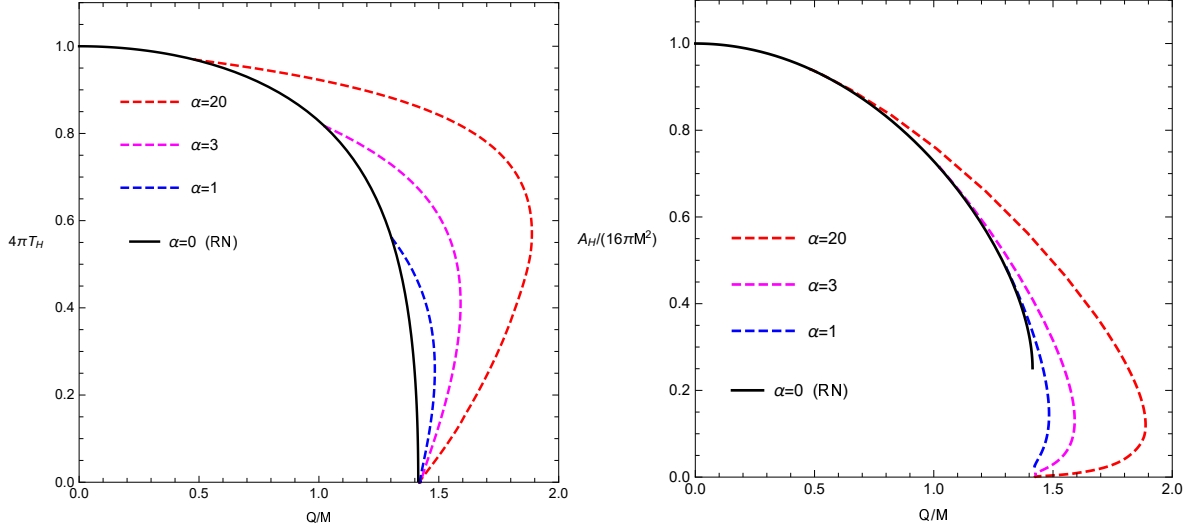


Figure 6: The temperature and horizon area as function of Q/M for the RN (solid lines) and hairy black holes with $\alpha = 1, 3, 20$ (dashed lines). Left: Temperature. Right: The ratio $A_H/16\pi M^2$.

in other theories (see e.g. refs. [15, 20, 21]). This property is however not sufficient to guarantee the stability of HBH; this would need a perturbative (or dynamical) analysis which is out of the scope of this paper.

Let us now discuss the critical phenomenon limiting the families of HBH while increasing $\phi(r_h)$. This can be understood from Fig.7. On the left, we show the metric functions $f(r), a(r)$ for the limiting configurations corresponding to $\alpha = 1$ and $\alpha = 20$ for the value of $\phi(r_h)$ very close to the critical value. The metric is characterized by two phenomena clearly appearing on the figure :

- A second horizon as seen by a second zero of the metric function $f(r)$ is approached for some

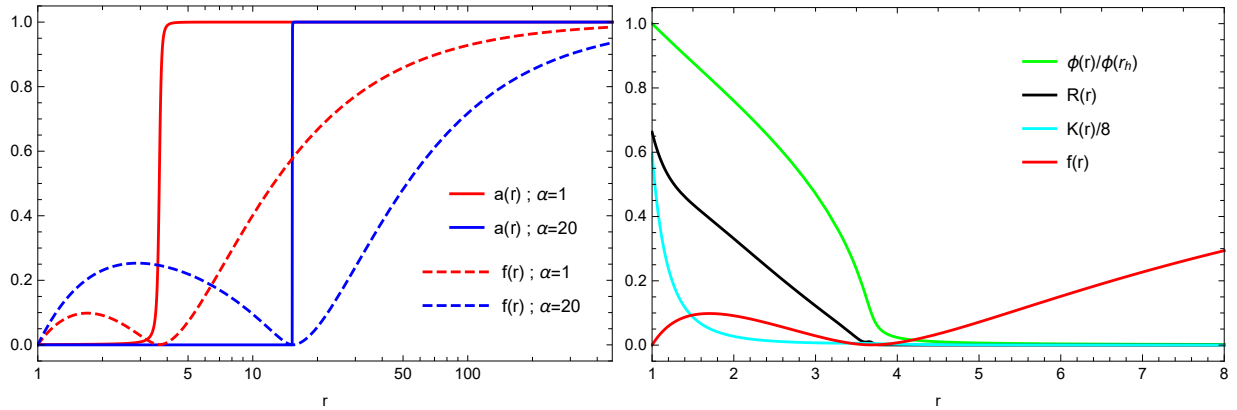


Figure 7: Left: Two profiles of the metric functions $f(r), a(r)$ for two critical HBH for $\alpha = 1, 20$ which turn into extremal RN solutions. Right: Profiles of $f(r), \phi(r)$ and the Ricci and Kretschmann invariants for the limiting configuration corresponding to $\alpha = 1$.

radius r_c (depending on α) such that $r_c > r_h$. The horizon r_c is extremal. Outside this horizon, the scalar field tends to null function and the metric approaches an extremal RN black holes.

- The function $a(r)$ is very small for $r \in [r_h, r_c]$ and raises steeply to $a(r) = 1$ for $r > r_c$.

The fact that all branches of HBH solutions terminates at $Q/M \sim \sqrt{2}$ on Fig.6 is then clear since the asymptotic charges (Mass and electric charge) of the HBH in this limit corresponds to the ones of an extremal RN solutions. Furthermore it was checked numerically that the temperature of the HBH tends to zero in the critical limit. Confirming the above statement, we present at the right hand side of Fig.7 the profiles of the Ricci and Kretschmann invariants R, K as well as the scalar field $\phi(r)$ for the case $\alpha = 1$. All these quantities are very close to zero for $r > r_c$. Furthermore, the invariants R, K are finite everywhere including the horizon r_h in spite of the fact that the value $a(r_h)$ becomes very small. We noticed a similar phenomenon for charged boson stars in a scalar-tensor Horndeski theory of the ‘‘John type’’ [26] where in certain circumstances a boson star loses its scalar hair and turns into an extremal RN black hole.

It is worth emphasizing that the pattern of HBH in the present model is, up to our knowledge, different from any other HBH present in the literature. In particular these are characterized by a single branch in the $Q/M, A_H/M^2$ plane and terminate into a singular configuration.

6 Summary

We have discovered a new type of scalarized charged black holes in a surprisingly simple system: The Einstein-Maxwell-Klein-Gordon Lagrangian, supplemented by a non-minimal coupling issued for the general vector-tensor theory formulated by G. Horndeski. Several kinds of new compact objects, including soliton-like and black holes with scalar hair, were constructed by using a spherically symmetric ansatz for the fields. In particular, the families of hairy black holes are constructed presenting different features from solutions constructed in various existing extended gravity models.

This system deserves a further study in various directions like the thermodynamic properties of these new hairy black holes, their angular and/or radial excitations and the solutions with asymptotically non-vanishing scalar field which we found to exist. Other types of compact objects, like boson stars, exist also when the scalar field becomes complex and massive. These directions as well as others are currently under investigation.

Acknowledgments : Y.B. gratefully acknowledges the Physics Division at the Open University of Israel in Raanana, for hospitality during an invited visit where this work was initiated. Support from the Research Authority of the Open University of Israel is also acknowledged.

References

- [1] G. W. Horndeski, Int. J. Theor. Phys. **10** (1974) 363.
- [2] G. W. Horndeski, J. Math. Phys. **17** (1976) 1980.
- [3] J. D. Bekenstein, Phys. Rev. Lett. **28** (1972) 452.

- [4] C. Teitelboim, *Lett. Nuovo Cim.* **3S2** (1972) 397.
- [5] J. D. Bekenstein, *Phys. Rev. D* **51** (1995), R6608.
- [6] C. A. R. Herdeiro and E. Radu, *Phys. Rev. Lett.* **112** (2014) 221101.
- [7] C. A. R. Herdeiro and E. Radu, *Int. J. Mod. Phys. D* **24** (2015), 1542014
- [8] T. P. Sotiriou, *Class. Quant. Grav.* **32** (2015), 214002
- [9] M. S. Volkov, arXiv:1601.08230 [gr-qc].
- [10] A. Nicolis, R. Rattazzi and E. Trincherini, *Phys. Rev. D* **79** (2009) 064036.
- [11] C. Deffayet, X. Gao, D. A. Steer and G. Zahariade, *Phys. Rev. D* **84** (2011) 064039
- [12] T. P. Sotiriou and S. Y. Zhou, *Phys. Rev. Lett.* **112** (2014) 251102
- [13] T. P. Sotiriou and S. Y. Zhou, *Phys. Rev. D* **90** (2014) 124063
- [14] D. D. Doneva and S. S. Yazadjiev, *Phys. Rev. Lett.* **120** (2018), 131103
- [15] H. O. Silva, J. Sakstein, L. Gualtieri, T. P. Sotiriou and E. Berti, *Phys. Rev. Lett.* **120** (2018), 131104
- [16] G. Antoniou, A. Bakopoulos and P. Kanti, *Phys. Rev. Lett.* **120** (2018), 131102.
- [17] P. Kanti, N. E. Mavromatos, J. Rizos, K. Tamvakis and E. Winstanley, *Phys. Rev. D* **54** (1996) 5049
- [18] P. Kanti, B. Kleihaus and J. Kunz, *Phys. Rev. D* **85** (2012) 044007
- [19] G. Antoniou, A. Bakopoulos, P. Kanti, B. Kleihaus and J. Kunz, *Phys. Rev. D* **101** (2020), 024033
- [20] C. A. R. Herdeiro, E. Radu, N. Sanchis-Gual and J. A. Font, *Phys. Rev. Lett.* **121** (2018), 101102
- [21] P. G. S. Fernandes, C. A. R. Herdeiro, A. M. Pombo, E. Radu and N. Sanchis-Gual, *Class. Quant. Grav.* **36** (2019), 134002 ; Erratum: *Class. Quant. Grav.* **37** (2020), 049501.
- [22] F. Muller-Hoissen and R. Sippel, *Class. Quantum Gravity*, **5** (1988) 1473.
- [23] G. Antoniou, A. Bakopoulos and P. Kanti, *Phys. Rev. D* **97** (2018), 084037.
- [24] Y. Brihaye and B. Hartmann, *Phys. Lett. B* **792** (2019) 244
- [25] U. Ascher, J. Christiansen, R. D. Russell, *Math. Comp.* **33** (1979) 659; U. Ascher, J. Christiansen, R. D. Russell, *ACM Trans.* **7** (1981) 209.
- [26] Y. Verbin and Y. Brihaye, *Phys. Rev. D* **97**, no. 4, 044046 (2018).